



Detection of Indoor Building Lighting Fixtures in Point Cloud Data using SDBSCAN

Humairah Mansor*, Shazmin Aniza Abdul Shukor*(C.A.), Razak Wong Chen Keng** and Nurul Syahirah Khalid*

Abstract: Building fixtures like lighting are very important to be modelled, especially when a higher level of modelling details is required for planning indoor renovation. LIDAR is often used to capture these details due to its capability to produce dense information. However, this led to the high amount of data that needs to be processed and requires a specific method, especially to detect lighting fixtures. This work proposed a method named Size Density-Based Spatial Clustering of Applications with Noise (SDBSCAN) to detect the lighting fixtures by calculating the size of the clusters and classifying them by extracting the clusters that belong to lighting fixtures. It works based on Density-Based Spatial Clustering of Applications with Noise (DBSCAN), where geometrical features like size are incorporated to detect and classify these lighting fixtures. The final results of the detected lighting fixtures to the raw point cloud data are validated by using F1-score and IoU to determine the accuracy of the predicted object classification and the positions of the detected fixtures. The results show that the proposed method has successfully detected the lighting fixtures with scores of over 0.9. It is expected that the developed algorithm can be used to detect and classify fixtures from any 3D point cloud data representing buildings.

Keywords: Clustering, Fixtures, Heuristic, Point Cloud Data, Segmentation.

1 Introduction

OBJECT detection from point cloud data has been extensively studied to achieve certain tasks for various applications. This includes the detection of humans [1], vehicles [2], and other important objects in respective areas [3], [4], [5]. It is often accompanied by point cloud segmentation, a process that involves grouping the points based on similar low-level attributes.

This process enables the analysis to classify or recognize objects by focusing on a smaller subset of

data, which can significantly reduce both the complexity and size of the dataset. The data size can be further reduced by modeling these objects for advanced analyses, resulting in simplified models instead of more complex point clouds [6], [7], [8], [9]. The high-quality point clouds generated by modern laser scanner or LIDAR can be used for information extraction about objects, such as buildings. Its applications have somewhat replaced traditional surveying methods, as it can significantly accelerate fieldwork.

The advent of LIDAR technology has been widely utilized in urban planning, environmental monitoring, telecommunications, and disaster mitigation [10]. In building monitoring, the present-time solution nowadays consists of fixing a LIDAR or 3D Terrestrial Laser Scanner (TLS) at building spaces and to survey the surrounding landscape. Architects and engineers used the 3D modelling, which may be part of Building Information Modelling (BIM), to illustrate how the building looks like to the owner and contractors before any renovation or reconstruction is done. The 3D model is then used by the contractors and can later be used by

Iranian Journal of Electrical & Electronic Engineering, 2025.
 Paper first received 31 Dec. 2024 and accepted 20 Feb. 2025.
 * The authors are with the Faculty of Electrical Engineering & Technology and Centre of Excellence for Intelligent Robotics & Autonomous Systems, Universiti Malaysia Perlis, 02600 Arau, Perlis, Malaysia.
 E-mails: humairah@unimap.edu.my, shazmin@unimap.edu.my, syahirahkhalid@unimap.edu.my.

** The author is with the Geodelta Systems Sdn. Bhd., 22, Jalan SS 20/11, Damansara Utama, Petaling Jaya 47400, Malaysia.
 E-mail: razwong@geodelta-systems.com.
 Corresponding Author: Shazmin Aniza Abdul Shukor.

the owners and managers for maintenance purposes [11]. Therefore, the development of digital information of BIM, consisting of the mechanical, electrical, plumbing (MEP) system in every building is very important to ensure accurate information and to reduce the time taken using hard copies. The digital system can be used to monitor, as well as localize the problematic components and regular maintenance [12].

1.1 Research Gaps

Most of the previous research in Architecture / Engineering / Construction (AEC) applications involves the detection of big, obvious structures like windows, doors, and furniture. The automatic processing of 3D point clouds can be speedy and efficient; however, the vast amount of data generated, and the time required to convert this data into useful information necessitate an appropriate method, especially when dealing with small and complex structures [14]. Current studies show that very few well-scalable features have been conducted to recognize huge components and small sizes components in the buildings at the same time. Usually, fixtures components such as lighting, piping, electrical boxes and sockets are neglected during the extraction process [15]. As a result, a geometry information extraction method for small-sized components is still lacking. This research fills in the gaps by exploring the combination of methods used in segmentation, which involves the extraction of small structures, specifically the lighting fixtures in the building using the size of the fixture's clusters. A suitable method to process a dense point cloud is explored to reduce the complexity of the data. This is to ensure that only the desired area of the point cloud data is processed, and the data is compatible with the processor of the laptop.

2 Methodology

2.1 Overall Flow Process

The overall process consists of: 1) data acquisition, 2) plane segmentation to simplify the dense point cloud data, 3) object detection and classification, and 4) evaluation of the proposed methods. Point cloud data collection is conducted at the laboratories in the Faculty of Electrical Engineering & Technology (FKTE), Universiti Malaysia Perlis, Malaysia, with the help of experts from Geodelta Systems Sdn. Bhd, Selangor. The type of lighting fixture that will be detected is the LED parabolic troffer with dimensions 60.96cm (length) x 30.48cm (width) and 7.62cm (height) which is commonly found at laboratories and corridors at FKTE. The laser scanner used in this project is Leica RTC360. MATLAB R2022b is used as the software tool to develop the system. The actual figure of the lighting fixture is shown in Fig. 1.



Fig 1. Actual figure of lighting fixtures

From the input data acquisition, a process called plane segmentation is applied. The segmentation process uses RANdom SAmple Consensus (RANSAC) algorithm. The process is carried out to minimize the size of dense raw point cloud data captured by a laser scanner, which aids in more efficient pre-processing and speeds up the whole process.

In order to detect clusters belonging to lighting fixtures, a model fitting method combined with DBSCAN is proposed, namely Size Density-Based Spatial Clustering of Application with Noise (SDBSCAN). From the clusters, the SDBSCAN is applied to determine the clusters that match the size of the lighting fixtures and removes the non-fixture clusters. The matched clusters are the detected lighting fixtures in the building. The performance of the proposed method is then assessed using appropriate parameters. Fig. 2 illustrates the flowchart of the proposed method.

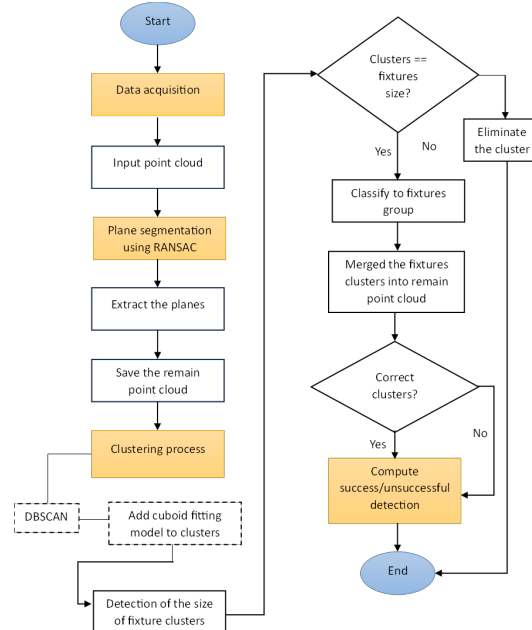


Fig 2. Flowchart of the proposed method

2.2 Plane Segmentation

Since the area of interest is the ceiling of the building, the top plane which is the ceiling needs to be segmented out to filter out the unnecessary data. Region of Interests (ROI) of the ceiling is extracted to minimize the size of the input point cloud. After that, RANSAC is applied to extract the top planes of the point cloud data. RANSAC algorithm classified the point cloud into inliers and outliers point cloud. The inliers are considered the planes and the outliers are the remaining point cloud data that will be used to detect and classify the object in point cloud. In general, RANSAC is used to define certain point cloud subgroups in point cloud data [16]. Every plane in 3D point cloud data can be represented by Eq. (1):

$$ax + by + cz + d = 0 \quad (1)$$

where x , y , and z are the coordinates of point in the space, while a , b and c represent the parameters of normal vector and d is the scalar product of normal vector. The distance D of point cloud data from the plane is calculated as in Eq. (2):

$$D = \frac{|ax + by + cz + d|}{\sqrt{a^2 + b^2 + c^2}} \quad (2)$$

where points that are less than maximum distance D and within normal vectors [a,b,c] are considered as the inliers data. The remaining point cloud data are considered as the outliers. The inliers that are extracted from the raw point cloud data are considered as the top plane.

2.3 Point Cloud Clustering

There are several methods introduced over the years, such as k-means, mean shift, DBSCAN, and Euclidean cluster. In this research, the proposed method is a hybrid segmentation, where the model fitting method and DBSCAN are combined to segment the point cloud data. The algorithm starts with clustering the remaining point cloud from the plane segmentation process before. There are three types of points identified by DBSCAN, which are the core point, border point, and noise point. To develop a cluster, two important parameters are used, which are the minimum points to form a cluster ($minPts$) and epsilon (ϵ) value which is the maximum distance between two points in the same cluster. From Artur Starzewski et.al. [17], the definition of epsilon (ϵ) neighborhood (N_ϵ) of object p in dataset D of point cloud equal to Eq. (3):

$$N_\epsilon(p) = \{q \in Ds | \text{dist}(p, q) \leq \epsilon\} \quad (3)$$

where:

- $N_\epsilon(p)$ is the ϵ neighbourhood of object p in dataset Ds .

- p is the core point if number of points belongs to $N_\epsilon(p)$ is greater than or equal to $minPts$.
- $\text{dist}(p, q)$ is the distance between object p and q in dataset Ds .
- Point q is *directly ϵ -reachable* from point p (for the given ϵ and the $minPts$) if p is the *core point* and q belong to $N_\epsilon(p)$.
- Point q is a *border point* if it is ϵ -reachable from point p (for the given ϵ and the $minPts$) and the number of points belong to $N_\epsilon(q)$ is smaller than the $minPts$.
- Point q is considered *noise* if it is neither a core point nor a border point.
- Point q is ϵ -reachable from point p (given ϵ and the minimum number of points, $minPts$) if they are connected through a sequence of core points, q_1, q_2, \dots, q_n , where $q_1=p$, $q_n=q$, and each subsequent point q_{i+1} is directly density-reachable from q_i .
- Point q is ϵ -connected to point p (given ϵ and $minPts$) if both points p and q are density-connected to a common point, o .

From the definition, the derivation of the cluster (C) of DBSCAN is as in Eq. (4) and Eq. (5):

- $\forall p, q \in Ds: \text{if } p \in C \text{ and } p \text{ is } \epsilon \text{ -reachable to point } q, \text{ (for the given } \epsilon \text{ and the } minPts \text{) then } q \in C$ (4)

- $\forall p, q \in C; p \text{ is } \epsilon \text{ -connected to } q \text{ (for the given } \epsilon \text{ and the } minPts \text{)}$ (5)

2.4 Size Density Based Spatial Clustering of Applications with Noise (SDBSCAN)

The execution of DBSCAN produced clusters from the points in the datasets. The remaining points will produce other clusters when the DBSCAN is executed again by next ϵ value. The $minPts$ is set to more than 3 to form every possible cluster [18]. Since DBSCAN produced many clusters, we proposed Size Density Based Spatial Clustering of Applications with Noise (SDBSCAN) with an ability to determine the size of the clusters produced and recognized the clusters which belongs to lighting fixtures and piping fixtures. There are three steps involved in developing the SDBSCAN:

- Determination of the appropriate $minPts$ and ϵ value to form a cluster.
- Determination of cluster size range which represents the lighting fixtures.
- Elimination of clusters which do not meet the size of the fixtures.

To develop a cluster, two important parameters are used, which are the minimum points to form a cluster ($minPts$) and epsilon (ϵ) value which is the maximum distance between two points in the same cluster [17]. The minimum points to form a cluster are based on the size of the input point cloud data. Larger datasets contribute to the larger $minPts$. Generally, the estimated value of minimum points is equal to the following Eq. (6):

$$minPts = 2 \times dim \quad (6)$$

where dim equals the dimension of the input point cloud data [19]. The larger value of minimum points is required for large and noisy datasets to reduce the amount of noise. Since the input point cloud data for all datasets are dense and very large, the $minPts$ of the training data is set to 100 [8]. The value is chosen based on several trials and testing with the most significant clusters produced.

The value of epsilon (ϵ) is determined by using a k-distance graph plot of the input data. The k-distance graph displays the average distance to the k -th nearest neighbor for each point in the input data, where k is the value of $minPts$ chosen beforehand. The ideal value of ϵ is the value at the elbow of the k-distance graph, which represents the optimum value to cluster the input point cloud [20]. By using MATLAB, the k-distance graph is generated by calculating pairwise distances D between two sets of observation, which is the $minPts$ and Euclidean distances. Fig. 3 shows the k-distance graph of Lab C2 and the value of ϵ equal to 0.10. Therefore, the value will be used in programming execution.

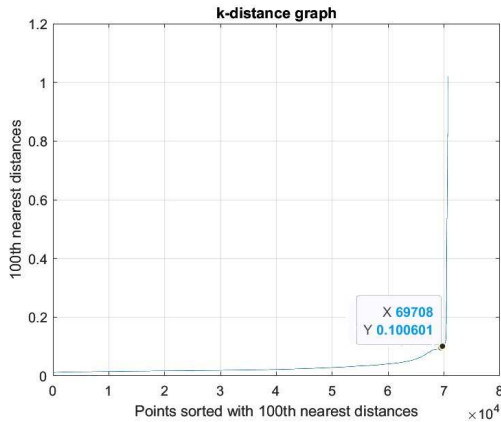


Fig. 3 K-distance graph for Lab C2

A model-fitting segmentation method is employed to determine the cluster size by creating a cuboid model and fitting a bounding box around the point cloud. The cuboid model of a point cloud contains parameters of the object, which is the center of the object $[x_{ctr}, y_{ctr}, z_{ctr}]$, the length of the cuboid $[x_{len}, y_{len}, z_{len}]$ along x-, y-, and z-axis, and the rotation angle of the object in

degrees along x-, y-and z-axis. The parameters of the cuboid model are shown in Fig. 4.

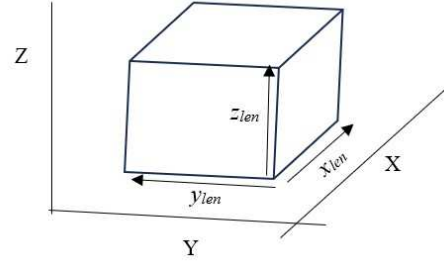


Fig. 4 Cuboid model for lighting fixtures

To detect the cluster that belongs to the lighting fixtures, the SDBSCAN process is improved with cluster size checking after the formation of clusters. Each cluster obtained from DBSCAN is fitted with cuboid model to determine lighting fixture clusters. The size of the clusters is based on the threshold value which is the difference of minimum and maximum value of x-axis, y-axis and z-axis which represents the wide, length and height of the cuboid model. The calculation of the difference of x-axis length is given by $x_{max} - x_{min}$, y-axis length is $y_{max} - y_{min}$, and z-axis length is $z_{max} - z_{min}$ [20]. The values are based on the minimum value and maximum value of the differences. If the clusters fulfill the criteria of the threshold, the cluster model will be saved and displayed as the detected object. For any points equal to non-fixtures, the points are automatically discarded from the point cloud.

From Eq. (4) and Eq. (5), the derivation of the clusters for SDBSCAN (C_{fix}), are as in Eq. (7) and Eq. (8):

$$C_{fix} \in C \quad (7)$$

where:

$$C_{fix} = \{x \mid x_{min} \leq x_{len} \leq x_{max}\} \& \{y \mid y_{min} \leq y_{len} \leq y_{max}\} \& \{z \mid z_{min} \leq z_{len} \leq z_{max}\} \quad (8)$$

Therefore, to differentiate lighting fixtures clusters and non-lighting clusters, we derived the equation as in Eq. (9):

$$C_{fix} = \begin{cases} 0, C \notin C_{fix} \\ 1, C \in C_{fix} \end{cases} \quad (9)$$

where the condition in Eq. (9) discards all the clusters that do not belong to fixtures clusters and keeps only the fixtures clusters. The algorithm proposed has reduced the noise in the point cloud and can automatically detect and classify the building fixtures in the point cloud. The process continues until no points are left.

3 Results and Discussions

3.1 Plane Segmentation Results

Fig. 5 to Fig. 7 show the point cloud data of Lab C2 and the results of plane segmentation for the ceiling part until extraction of the top plane. Fig. 5 is the raw point cloud data from the laser scanner. The raw data is then converted to ASCII format using Cloud Compare. Only the ceiling view is considered to minimize the area of interest where the lighting fixtures exist as shown in Fig.6. Fig.7 shows the top plane that has been extracted from Fig.6 using RANSAC. The remaining point cloud data left will be used to detect the lighting fixtures in the point cloud.

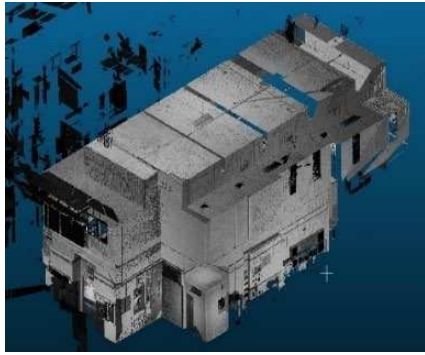


Fig. 5 Raw data of Lab C2

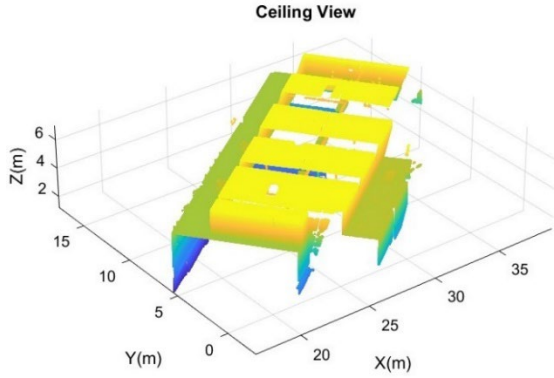


Fig. 6 Ceiling view of Lab C2

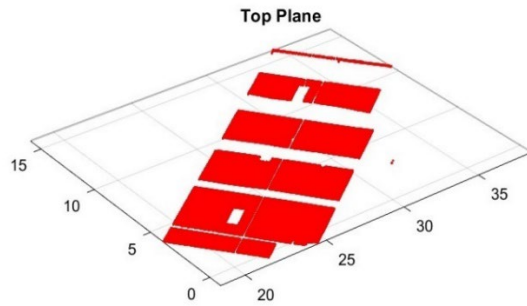


Fig. 7 Top plane extracted from ceiling view of Lab C2

3.2 Lighting Fixtures Detection Results

The remaining point cloud data are then processed to detect and classify the lighting fixtures. Fig. 8 and Fig. 9 shows the results of lighting fixture detection. SDBSCAN clustering is conducted to form clusters and detect the lighting fixtures in Fig. 8. DBSCAN and model-fitting method are combined, and the size of the clusters is determined. Fig.9 shows the results of SDBSCAN clustering. The result shows that the lighting fixtures were successfully detected, and all non-lighting fixture clusters were automatically removed from the point cloud data. The point cloud data is classified into lighting fixtures and non-lighting fixtures only. Therefore, all point cloud data that does not belong to the size will be on the same cluster.

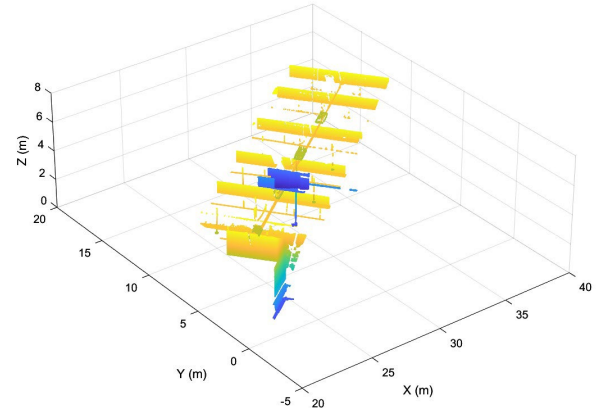


Fig. 8 Remain point cloud data after top plane extraction of Lab C2

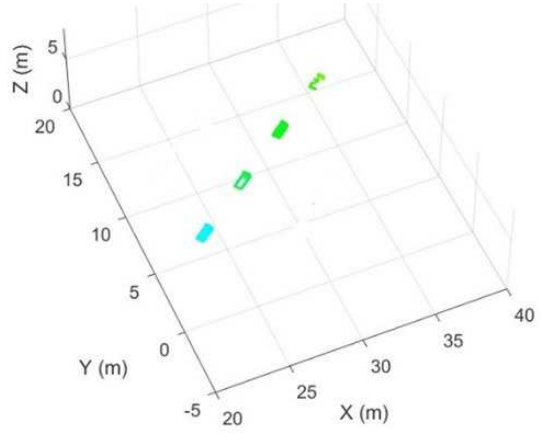


Fig. 9 Lighting fixtures detection in Lab C2 using SDBSCAN

To validate the proposed method, point cloud data of two more scenes, Lab A2 and Lab B2 of FKTE, are tested and the parameters are determined. The results of

Lab A2 are shown in Fig. 10 to Fig. 12, meanwhile results of Lab B2 are shown in Fig.13 to Fig.15.

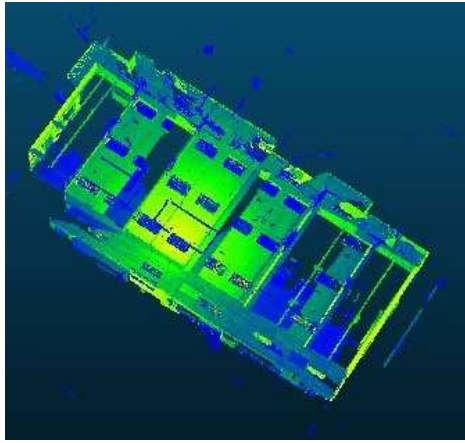


Fig. 10 Raw data of Lab A2

fixtures in the remaining point cloud data of Lab A2 and Lab B2.

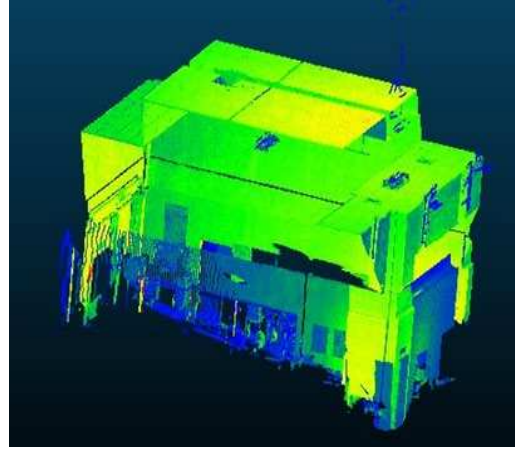


Fig. 13 Raw data of Lab B2

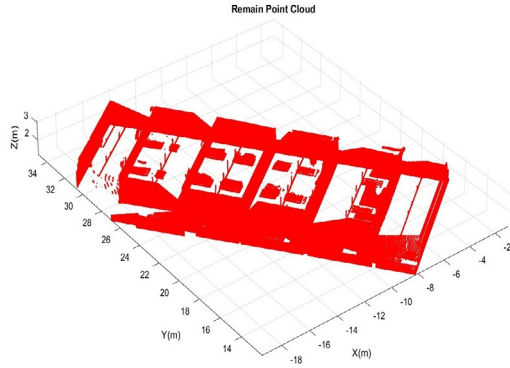


Fig. 11 Remain point cloud data after top plane extraction of Lab A2

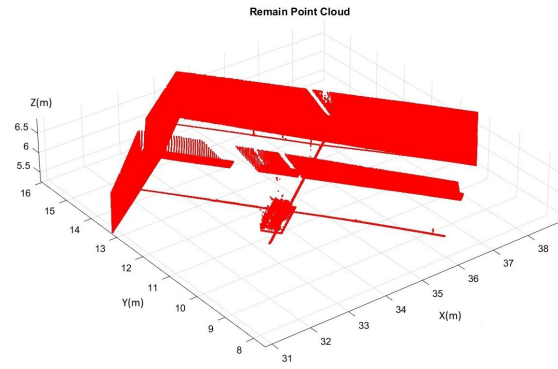


Fig.14 Remain point cloud data after top plane extraction of Lab B2

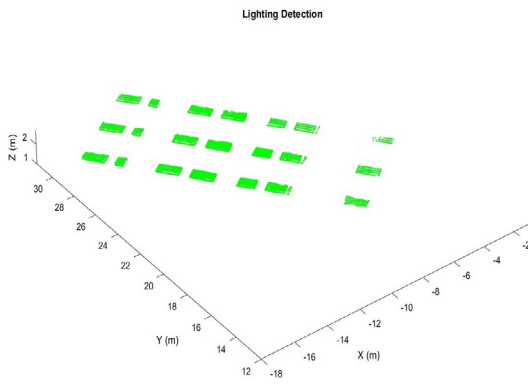


Fig. 12 Lighting fixtures detection in Lab A2 using SDBSCAN

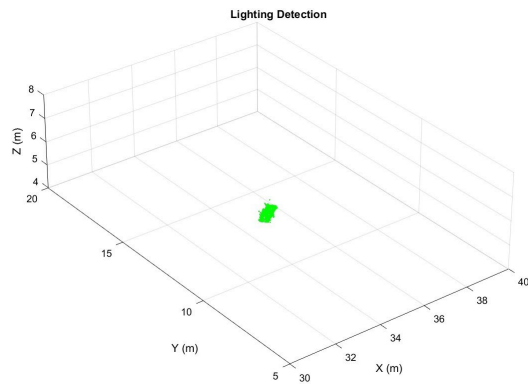


Fig.15 Lighting fixtures detection in Lab B2 using SDBSCAN

3.3 Evaluation of Performance

The proposed segmentation method for object detection and classification using SDBSCAN is

From the results, the proposed method has successfully detected and located the initial location of lighting

evaluated using two criteria: the correct classification of the predicted object in point cloud data to the ground truth and the accuracy of the predicted object to the ground truth.

Precision (P), Recall (R), and F1-Score [21] are used to calculate the correct classification of predicted objects in point cloud data to the ground truth. The conditions of the detected object involved three parameters, which are True Positive (TP) for the number of lighting fixtures correctly detected, False Negative (FN) for the number of lighting fixtures incorrectly detected, False Positive (FP) for no lighting fixtures exist but incorrectly detected as one and True Negative (TN) for all non-fixtures that are correctly detected as non-fixtures. The formulas for P, R, and F1-Score are shown in Eq. (10) to Eq. (12):

$$P = \frac{TP}{TP + FP} \quad (10)$$

$$R = \frac{TP}{TP + FN} \quad (11)$$

$$F1 - Score = 2 \times \frac{P \times R}{P + R} \quad (12)$$

Table 1 shows the tabulated predicted and actual confusion matrix according to TP, FP, and FN of Lab A2, Lab B2 and Lab C2. The ground truth data is done by manually counting the number of lighting fixtures that appear in point cloud data. The number of lighting fixtures identified in the point cloud data after the clustering process using SDBSCAN is represented by n clusters. The results are presented in Table 1, Table 2 and Table 3 which shows the predicted and actual confusion matrix of Lab A2, Lab B2, and Lab C2.

Table 1 Predicted and actual confusion matrix of Lab A2

$n = 21$	Actual =0(non-fixtures)	Actual=1(fixtures)
Predicted = 0 (non-fixtures)	TN=0	FP=0
Predicted=1(fixtures)	FN=0	TP=21

Table 2 Predicted and actual confusion matrix of Lab B2

$n = 1$	Actual =0(non-fixtures)	Actual=1(fixtures)
Predicted = 0 (non-fixtures)	TN=0	FP=0
Predicted=1(fixtures)	FN=0	TP=1

Table 3 Predicted and actual confusion matrix of Lab C2

$n = 4$	Actual =0(non-fixtures)	Actual=1(fixtures)
Predicted = 0 (non-fixtures)	TN=0	FP=0
Predicted=1(fixtures)	FN=0	TP=4

From the tables of predicted and actual confusion matrix, the F1-score is calculated. Table 4 shows the F1-Score of Lab A2, Lab B2 and Lab C2. From the table, the F1-score for all labs is 1, meaning that all the predicted objects are successfully identified as lighting fixtures in the point cloud.

Table 4 F1-score of Lab A2, Lab B2 and Lab C2

	P	R	F1-Score
Lab A2	1	1	1
Lab B2	1	1	1
Lab C2	1	1	1

Another method of evaluation is by using Intersection over Union (IoU). The IoU calculates the percentage of overlap between the predicted object to the ground truth. The formula for IoU is shown in Eq. (13):

$$IoU = \frac{|P \cap G|}{|P \cup G|} \quad (13)$$

where $|P \cap G|$ is the number of points in the intersection of the predicted and ground truth point cloud data between set P and set G and $|P \cup G|$ is the number of points in the union of the predicted and ground truth point cloud data of the sets. Table 5 below summarizes the IoU value for Lab A2, Lab B2 and Lab C2. The IoU score for Lab A2 is 0.99, Lab B2 is 0.98 and Lab C2 is 0.95. The higher IoU indicates more accurate object detection [22], [23]. Lab C2 scores lower scores compared to Lab A2 and Lab B2 due to the higher data loss during scanning process of the original point cloud. This leads to a lower percentage of detected objects to the ground truth point cloud data.

Table 5 IoU score for Lab A2, Lab B2 and Lab C2

Lab	IoU
A2	0.99
B2	0.98
C2	0.95

Lastly, the F1-score and IoU score for Lab A2, Lab B2 and Lab C2 using DBSCAN and SDBSCAN are compared. From the results shown in Table 6, the F1-Score using SDBSCAN is better for Lab A2 and Lab C2 compared to DBSCAN. This is because the DBSCAN

measures the clusters based on the minimum distances of point cloud data. Therefore, there are some of the lighting fixtures clustered into several parts due to the missing data points on the original point cloud. By using SDBSCAN, the clusters are measured by size, hence clusters that are within the range of the sizes are classified into the same clusters. The IoU score of Lab A2, Lab B2 and Lab C2 are compared using DBSCAN and SDBSCAN. The results show that the IoU score for Lab A2 and Lab C2 are slightly higher than the DBSCAN score. This is due to the separated clusters detected by DBSCAN that lower the percentage of overlap between detected object and ground truth. Based on the results, it can be concluded that the method performs effectively with the tested datasets.

Table 6 Comparisons of F1-score and IoU score for Lab A2, Lab B2 and Lab C2 using DBSCAN and SDBSCAN

Lab	F1- Score		IoU	
	DBSCAN	SDBSCAN	DBSCAN	SDBSCAN
A2	0.95	1	0.98	0.99
B2	1	1	0.98	0.98
C2	0.86	1	0.90	0.95

4 Conclusion

This research proposed an improved segmentation method for object detection in point cloud data, specifically lighting fixtures in indoor building, using the combination of DBSCAN and cuboid model fitting method namely SDBSCAN. The result of the research shows that the lighting fixtures are successfully identified in the building environment. The F1-Score and IoU scores are more than 0.9 which means that the method accurately detects and locates the initial location of the lighting fixtures in segmented point cloud data. For future work, improvements could focus on enhancing the process of removing unwanted noise from point cloud data, exploring alternative segmentation techniques, and conducting geometric part analysis for 3D object classification in cluttered and occluded scenes. The results could also be enhanced by employing alternative methods, such as deep learning algorithms, and expanding the work to handle more complex objects without simplifying the point cloud data.

Acknowledgment

This research was funded by Centre of Excellence for Intelligent Robotics & Autonomous Systems (CIRAS), Universiti Malaysia Perlis.

References

[1] Schlosser J., Christopher K. C., and Zsolt K. 2016. “Fusing LIDAR and Images for Pedestrian Detection Using Convolutional Neural Networks.” IEEE Xplore. May 1, 2016. <https://doi.org/10.1109/ICRA.2016.7487370>.

[2] Wang Y., Anttoni J., Juha H., Jouko L., Harri K., Antero K., Eetu P., and Hannu H. 2016. “Object Classification and Recognition from Mobile Laser Scanning Point Clouds in a Road Environment.” IEEE Transactions on Geoscience and Remote Sensing 54 (2): 1226–39. <https://doi.org/10.1109/tgrs.2015.2476502>.

[3] A.J., Jdeed. 2019. “Review of Point Clouds Segmentation and Classification Methods for Architectural Objects.”

[4] Fu H., Hao L., Yanqi D., Fu X., and Feixiang C. 2022. “Segmenting Individual Tree from TLS Point Clouds Using Improved DBSCAN.” Forests 13 (4): 566–66. <https://doi.org/10.3390/f13040566>.

[5] Huang Z., Yongcui W., Jie W., Peng W., and Xudong C. 2023. “An Object Detection Algorithm Combining Semantic and Geometric Information of the 3D Point Cloud.” Advanced Engineering Informatics 56 (April): 101971– 71. <https://doi.org/10.1016/j.aei.2023.101971>.

[6] Poux F., Mattes C., and Kobbelt L. . 2020. “Unsupervised Segmentation Of Indoor 3d Point Cloud: Application To Object-Based Classification.” The International Archives of the Photogrammetry, Remote Sensing and Spatial Information Sciences XLIV-4/W1-2020 (44): 111–18.

[7] Wijaya C., and Harintaka. 2023. “Analysis and Evaluation of PointNet for Indoor Office Point Cloud Semantic Segmentation.” International Journal on Advanced Science, Engineering and Information Technology/International Journal of Advanced Science, Engineering and Information Technology 13 (6): 2345–53. <https://doi.org/10.18517/ijaseit.13.6.18887>.

[8] Singh P.S., Iainehborlang M. N., Valarie M., Dibyajyoti C., Victor S., and S. P. Aggarwal. 2023. “Three-Dimensional Point Cloud Segmentation Using a Combination of RANSAC and Clustering Methods.” Current Science 124 (4): 434–41. <https://doi.org/10.18520/cs/v124/i4/434-441>.

[9] Nguyen A., and Bac L. 2013. “3D Point Cloud Segmentation: A Survey,” no. October 2015. <https://doi.org/10.1109/RAM.2013.6758588>.

[10] Bool D. L., Mabaquiao L. C., Tupas M. E. , and Fabila J. L. . 2018. “Automated Building Detection Using RANSAC from Classified LiDAR Point Cloud Data.” International Archives of the Photogrammetry, Remote Sensing and Spatial Information Sciences - ISPRS Archives 42 (4/W9):

115–21. <https://doi.org/10.5194/isprs-archives-XLII-4-W9-115-2018>.

[11] Isa S. N. M., Shazmin A. S, Rahim N.A , Maarof I , and Yahya Z. R . 2018. “A Review of Data Structure and Filtering in Handling 3D Big Point Cloud Data for Building Preservation.” 2018 IEEE Conference on Systems, Process and Control (ICSPC), no. June 2019: 141–46. <https://doi.org/10.1109/SPC.2018.8704136>.

[12] Wang R., Jiju P., and Dong C. 2018. “LiDAR Point Clouds to 3D Urban Models: A Review,” no. January. <https://doi.org/10.1109/JSTARS.2017.2781132>.

[13] Hu, Z., Pei-Long T., Sun-Wei L., and Jian-Ping Z. 2018. “BIM-Based Integrated Delivery Technologies for Intelligent MEP Management in the Operation and Maintenance Phase.” Advances in Engineering Software 115 (January): 1–16. <https://doi.org/10.1016/j.advengsoft.2017.08.007>.

[14] Adán A., Blanca Q., Samuel A. P., and Frédéric B. 2018. “Scan-to-BIM for ‘Secondary’ Building Components.” Advanced Engineering Informatics 37 (November 2017): 119–38. <https://doi.org/10.1016/j.aei.2018.05.001>.

[15] Wang B., Chao Y., Han L., Jack C.P. C., and Qian W. 2021. “Fully Automated Generation of Parametric BIM for MEP Scenes Based on Terrestrial Laser Scanning Data.” Automation in Construction 125 (February): 103615. <https://doi.org/10.1016/j.autcon.2021.103615>.

[16] Ma B., Can Y., Aihua L., Yuxue C., and Lihua C. 2023. “A Faster DBSCAN Algorithm Based on Self- Adaptive Determination of Parameters.” Procedia Computer Science 221 (January): 113–20. <https://doi.org/10.1016/j.procs.2023.07.017>.

[17] Starczewski A., Piotr G., and Meng J. E. 2020. “A New Method for Automatic Determining of the DBSCAN Parameters.” Journal of Artificial Intelligence and Soft Computing Research 10 (3): 209–21. <https://doi.org/10.2478/jaiscr-2020-0014>.

[18] Latifi-Pakdehi, Alireza, and Negin D. 2021. “DBHC: A DBSCAN-Based Hierarchical Clustering Algorithm.” Data and Knowledge Engineering 135 (April): 101922. <https://doi.org/10.1016/j.datak.2021.101922>.

[19] Ahmed K.N., and Abdul R.T. 2016. “An Overview of Various Improvements of DBSCAN Algorithm in Clustering Spatial Databases.” International Journal of Advanced Research in Computer and Communication Engineering 5 (2): 360– 63. <https://doi.org/10.17148/IJARCCE.2016.5277>.

[20] Chen H., Man L., Wanquan L., Weina W., and Peter X. L. 2022. “An Approach to Boundary Detection for 3D Point Clouds Based on DBSCAN Clustering.” Pattern Recognition 124. <https://doi.org/10.1016/j.patcog.2021.108431>.

[21] Sokolova M., Nathalie J., and Stan S. 2006. “Beyond Accuracy , F-Score and ROC: A Family of Discriminant Measures for Performance Evaluation Beyond Accuracy , F-Score and ROC : A Family of Discriminant Measures for Performance Evaluation,” no. January. <https://doi.org/10.1007/11941439>.

[22] Cowton J., Ilias K., and Jaume B. 2019. “Automated Individual Pig Localisation , Tracking And Behaviour Metric Extraction Using Deep Learning.” <https://doi.org/10.1109/ACCESS.2019.2933060>.

[23] Padilla R., Sergio L. N., and Eduardo A.B.S. 2020. “A Survey on Performance Metrics for Object- Detection Algorithms,” no. July. <https://doi.org/10.1109/IWSSIP48289.2020>

Biographies



Humairah Mansor is a Ph.D student and also a lecturer at Faculty of Electrical Engineering & Technology, Universiti Malaysia Perlis, Malaysia. She graduated with a Bachelor’s degree in Electrical (Electronics) Engineering from Universiti Malaysia Pahang Al-Sultan Abdullah in 2007 and obtained Master’s degree in Mechatronic Engineering from Universiti Malaysia Perlis in 2014. Her research interests include point cloud data, machine learning and robotics.



Shazmin Aniza Abdul Shukor is an Associate Professor from Mechatronic Engineering, Faculty of Electrical Engineering & Technology, Universiti Malaysia Perlis. She obtained her Ph.D. in Engineering from the University of Warwick, UK in 2013. Her research work includes LIDAR and point cloud data processing, towards various applications.



Razak Wong Chen Keng is a surveying equipment specialist in GPS and Terrestrial Laser Scanning (TLS). He completed his first degree in Surveying and Mapping Science in 1998 and Master of Business Administration in 2004. He is now the Director of Geodelta

Systems Sdn. Bhd., for which core business are in commercial TLS services, BIM / Scan to BIM; has interest in researching built environment, 3D visualization and virtual reality.



Nurul Syahirah Khalid is a Senior Lecturer at the Faculty of Electrical Engineering & Technology, Universiti Malaysia Perlis. She graduated with a Bachelor's degree in Mechatronics Engineering from Universiti Teknikal Malaysia Melaka in 2010. In 2012, she obtained her

Master's degree in Electrical Engineering (Mechatronics and Automation Control) from Universiti Teknologi Malaysia, Johor. She completed her PhD in Mechatronics Engineering at Universiti Malaysia Perlis in 2020. Currently, she is pursuing a Post-Doctoral research position at the University of Ghent, Belgium. Her research interests include sensor data fusion, machine learning, and control systems.